Non-classicality thresholds for multiqubit states - numerical analysis

Jacek Gruca,¹ Wiesław Laskowski,^{1,2,3,*} Marek Żukowski,¹ Nikolai Kiesel,⁴ Witlef Wieczorek,^{2,3,†} Christian Schmid,^{2,3,5} and Harald Weinfurter^{2,3}

¹Institute of Theoretical Physics and Astrophysics, University of Gdańsk, PL-80-952 Gdańsk, Poland ²Fakultät für Physik, Ludwig-Maximilians Universität München, D-80799 München, Germany ³Max-Planck Institut für Quantenoptik, D-85748 Garching, Germany ⁴Faculty of Physics, University of Vienna, A-1090 Vienna, Austria ⁵European Organisation for Astronomical Research in the Southern Hemisphere, D-85748 Garching, Germany (Dated: November 15, 2018)

States that strongly violate Bell's inequalities are required in many quantum-informational protocols as, for example, in cryptography, secret sharing, and the reduction of communication complexity. We investigate families of such states with a numerical method which allows us to reveal non-classicality even without direct knowledge of Bell's inequalities for the given problem. An extensive set of numerical results is presented and discussed.

I. INTRODUCTION

Until the discovery of the protocol of entanglement-based quantum cryptography [1], Bell's theorem was relevant only in discussions concerning foundations of quantum mechanics. It established means to evaluate the most reasonable class of hidden variable theories, i.e., local and realistic theories. Once the theorem proved useful in quantum cryptography and other quantum communication schemes (secret sharing [2], reduction of communication complexity [3–5], etc.), it gained an additional technical status. Today, we are not only interested in showing that given quantum correlations do not admit a local hidden variable model, but also, with Bell inequalities, we can now prove the usefulness of states in quantum protocols. The strength of such violations indicates resistance to noise or to decoherence.

However, only in simple cases, like two dichotomic measurements per observer, one can pinpoint the full set of such Bell-type inequalities, and put them into a manageable form of just one single non-linear inequality [6, 7]. In other cases we know usually only some subsets of tight inequalities for the given problem. These subsets still contain a vast number of different inequalities.

One of the methods to avoid the problem of both missing inequalities and handling the exploding numbers of known ones is to address the problem numerically, without a direct use of Bell's inequalities [8]. It is very easy to notice that the problem of existence of a local hidden variable model for the given set of quantum probabilities is a form of a linear programming problem (see Sec. II). Thanks to such an approach it was possible to show for example that non-classicality of two-qudit correlations is higher than for qubits, and that it increases with the dimension [9].

Below we present how linear programming can be harnessed to study non-classicality of quantum correlations. This approach was put in the form of a computer code: Steam-roller. We will present the numerical results in Secs. III and IV. Here we particularly aimed at multi-setting scenarios for multi-qubit states which are known to possess interesting kinds of non-classical behavior. Most of our results cover regions for which the full set of Bell's inequalities is unknown. Even the results for two settings per observer cover a new territory: they are produced for the full set of probabilities for the given N-gubit problem. In the case of the WWWZB inequalities [6, 7, 10] only highest order correlation functions [11] are taken into account. These do not reflect interference effects that may occur between subsets of particles. Thus the WWWZB set, despite being complete for highest order correlation functions (in the case of a two setting choice per observer), is not complete for the full description of quantum phenomena. This full set of probabilities for the given problem gives full knowledge about an experiment, and therefore contains all available information.

II. LINEAR PROGRAMMING

In the most general Bell's experiment, N observers perform measurements on a given state ρ_N . Each observer can choose between m_i arbitrary dichotomic observables $(i=1,\ldots,N)$. Their measurement results will exhibit correlations, not describable by classical statistics (i.e., by classical realistic models). For brevity let us consider a case with two observers (Alice and Bob) and two measurement settings per side. In this case the local realistic models are equivalent to the existence of a joint probability distribution $p_{lr}(a_1, a_2, b_1, b_2)$, where $a_i = \pm 1$ denotes the result of the measurement of Alice's i-th observable (Bob's results are denoted by $b_k = \pm 1$). Quantum predictions for the probabilities are the marginal sums of the

^{*} wieslaw.laskowski@univ.gda.pl

[†] Present address: Faculty of Physics, University of Vienna, Boltzmanngasse 5, A-1090 Wien, Austria

above joint probability distribution p_{lr}

$$P_{QM}(r_a, r_b | A_1, B_1) = \sum_{a_2, b_2 = \pm 1} p_{lr}(r_a, a_2, r_b, b_2)$$

$$P_{QM}(r_a, r_b | A_1, B_2) = \sum_{a_2, b_1 = \pm 1} p_{lr}(r_a, a_2, b_1, r_b)$$

$$P_{QM}(r_a, r_b | A_2, B_1) = \sum_{a_1, b_2 = \pm 1} p_{lr}(a_1, r_a, r_b, b_2)$$

$$P_{QM}(r_a, r_b | A_2, B_2) = \sum_{a_1, b_1 = \pm 1} p_{lr}(a_1, r_a, b_1, r_b), \quad (1)$$

where $P_{QM}(r_a, r_b|A_i, B_k)$ denotes the probability of obtaining the result r_a by Alice and r_b by Bob, when they measure the observables A_i and B_k , respectively. It has been shown that for some entangled states, no local realistic probability distribution $p_{lr}(a_1, a_2, b_1, b_2)$ exists, which could satisfy the set of equalities (1). Therefore, no local realistic model can reproduce the predictions of quantum mechanics for these entangled states. This statement is known as Bell's theorem [12].

This is one of the ways one can express Bell's theorem. The more frequent approach is to find certain (Bell) inequalities which are satisfied by local realistic models, but violated by some quantum predictions. More importantly, there are many statements on the "strength" of a violation of such inequalities which use such terms as "amount of violation" or "factor of violation." However, such measures cannot be used for direct comparison between different Bell inequalities or with a different method, such as the one used in our paper. Thus, following [9], we shall use a "violation" parameter v_{crit} which seems to be much more objective: we shall seek the amount of random ("white") noise admixture that is required to completely hide the non-classical character of the original correlations for the given state.

If we mix some amount of white noise to the two-qubit state ρ , we obtain a state described by the following density operator:

$$\rho(v) = v\rho + \frac{1 - v}{2^2} \mathbb{1}^{\otimes 2}.$$
 (2)

The quantum probability $P_{QM}^{v}(r_a, r_b|A_i, B_k) \equiv P(r_a, r_b|A_i, B_k)$ for the state $\rho(v)$ reads

$$P(r_a, r_b | A_i, B_k) = v P_{QM}(r_a, r_b | A_i, B_k) + \frac{1}{2^2} (1 - v).$$
 (3)

The parameter v is the visibility of the state, and obviously (1-v) is the amount of noise admixture. For v=0 the equalities (1) are obviously satisfied (white noise has a local realistic model). For v=1 the equalities (1) can not be satisfied for some entangled states ρ (and for a particular choice of observables). For such states there exists the critical visibility v_{crit} that for $v \leq v_{crit}$ there exists a local realistic probability distribution $p_{lr}(a_1, a_2, b_1, b_2)$ that satisfies the set of equalities (1).

A set of 16 probabilities $P_{QM}(r_a, r_b|A_i, B_k)$ corresponds to a single point in a 16-dimensional space. Those sets which can be described using local realistic models form a convex geometric figure called a Bell-Pitovsky polytope in this 16-dimensional space. The facets of the polytope are equivalent to tight Bell inequalities. For $v = v_{crit}$ the local realistic probabilities $p_{lr}(a_1, a_2, b_1, b_2)$ lead to a set of probabilities $P_{QM}(r_a, r_b | A_i, B_k)$ which form the coordinates of a geometric point which lies in a facet of the polytope (i.e., they saturate a Bell inequality). It has to be noted, however, that our numerical method does not lead to uncovering particular Bell inequalities which are violated by an investigated state. We think that, the power of the method lies in the fact that one does not need any knowledge at all of the forms of Bell inequalities when analyzing non-classicality of quantum-entangled states. Seeking violated Bell inequalities is highly inefficient, since even in the simplest cases one ends up with an exploding number of Bell inequalities, the bulk of them trivial. We skip this cumbersome step entirely, see the following paragraphs.

As mentioned, critical visibility v_{crit} depends on the particular set of observables Alice and Bob choose from. We can parametrize any dichotomic observable X_i by the two angles θ_i^X and ϕ_i^X (X = A, B) in the following way:

$$X = |+\rangle_X \langle +|-|-\rangle_X \langle -|,$$

$$|\pm\rangle_X = \cos(\pm \pi/4 + \theta_i^X)|0\rangle_X + e^{i\phi_i^X} \sin(\pm \pi/4 + \theta_i^X)|1\rangle_X.$$
(4)

Now, the quantum probability can be calculated: $P_{QM}(r_a, r_b|A_i, B_k) = \text{Tr}(\rho|r_a\rangle_A\langle r_a|\otimes|r_b\rangle_B\langle r_b|)$. Hence we can define the critical visibility function of the angles

$$v_{crit}(\theta_1^A, \phi_1^A, \theta_2^A, \phi_2^A, \theta_1^B, \phi_1^B, \theta_2^B, \phi_2^B) \in [0, 1].$$
 (5)

Our task is to find, for a given state ρ , the minimal critical visibility. If the two observers A and B perform two measurements each, the probabilities (3) are then parametrized by the angles:

$$P(r_a, r_b | A_i, B_k) \equiv P(r_a, r_b, \theta_i^A, \phi_i^A, \theta_k^B, \phi_k^B). \tag{6}$$

The critical visibility is obtained by maximization of the visibility until the set of equalities (1) can no longer be satisfied. This is done by means of linear programming. We adopt

$$p_0 \equiv p_{lr}(-, \dots, -, -),$$

$$p_1 \equiv p_{lr}(-, \dots, -, +),$$

$$\dots$$

$$p_{n-1} \equiv p_{lr}(+, \dots, +, +),$$
(7)

where $n = 2^{m_1 + \dots + m_N}$ and hereby give a complete description of the linear programming problem to be solved (based on Eqns. (1) and (3)) for the case with Alice and Bob:

$$\sum_{a_2,b_2=\pm 1} p_{lr}(r_a, a_2, r_b, b_2) = \frac{1-v}{2^2} + vP(r_a, r_b, \theta_1^A, \phi_1^A, \theta_1^B, \phi_1^B),$$

$$\sum_{a_2,b_1=\pm 1} p_{lr}(r_a, a_2, b_1, r_b) = \frac{1-v}{2^2} + vP(r_a, r_b, \theta_1^A, \phi_1^A, \theta_2^B, \phi_2^B),$$

$$\sum_{a_1,b_2=\pm 1} p_{lr}(a_1, r_a, r_b, b_2) = \frac{1-v}{2^2} + vP(r_a, r_b, \theta_2^A, \phi_2^A, \theta_1^B, \phi_1^B),$$

$$\sum_{a_1,b_1=\pm 1} p_{lr}(a_1, r_a, b_1, r_b) = \frac{1-v}{2^2} + vP(r_a, r_b, \theta_2^A, \phi_2^A, \theta_2^B, \phi_2^B),$$

$$\sum_{a_1,b_1=\pm 1} p_{lr}(a_1, r_a, b_1, r_b) = \frac{1-v}{2^2} + vP(r_a, r_b, \theta_2^A, \phi_2^A, \theta_2^B, \phi_2^B),$$

$$\sum_{b=0}^{n-1} p_{b} = 1; \quad 0 \le v \le 1; \quad 0 \le p_{b} \le 1,$$

$$z(p_0, p_1, \dots, p_{n-1}, v) = v,$$

$$(8)$$

where z is the (trivial) function to be maximized.

In the general case the four expressions above evaluate to $c=2^Nm_1\cdots m_N$ equalities (e.g. for 3 qubits and 6 measurement settings per side, there are 1728 equalities). The above is known as the canonical form of the linear programming problem. We use the revised simplex method [13] from the GNU Linear Programming Kit [14] to solve this problem. The top constraints form a simplex in the (n+1)-dimensional space spanned by p_0,\ldots,p_{n-1} and v. The algorithm traverses the vertices of the simplex until it finds the optimal solution. The returned solution is the global maximum of z – the critical visibility we seek. The minimization over the angles $\theta_1^A, \phi_1^A, \theta_1^B, \phi_1^B, \theta_2^A, \phi_2^A, \theta_2^B, \phi_2^B$ is realized by the downhill simplex method [15] from the SciPy package [16].

Please note that the complexity of the linear programming problem is defined by n and c – values which increase exponentially with the number of observers N or the number of settings m_i per observer. We are, therefore, limited to the computational capabilities of today's numerical machines when solving this problem. We used a machine with an Intel Pentium D CPU 3.20GHz processor for our computations. Some of the results in this paper took several weeks to compute. Computations of results for bigger problems can be anticipated to complete in a reasonable time when using faster machines in the future.

One might wonder about the credibility of the results presented in this paper. There are two aspects which raise doubts, namely, numerical precision and local minimum risk when computing the minimum of the critical visibility function. Please note that there is no local maximum risk when computing the value of the critical visibility function - the simplex algorithm guarantees it will always find the global maximum as described in [13]. As for the precision of the results, we will not conduct an extensive analysis but will plainly state that this is not an issue. For all the results which can be calculated analytically, STEAM-ROLLER generated results are compliant on all 14 displayed significant digits. For example, for a

two-qubit Greenberger-Horne-Zeilinger (GHZ) state, the analytically-derived minimal critical visibility is $\frac{\sqrt{2}}{2}$ and STEAM-ROLLER gives 0.70710678118655. One of the reasons for such outstanding precision is that the numerical errors do not propagate between consecutive critical visibility function invocations. Another is that the linear programming library used properly handles numerical instabilities. The local minimum risk when computing the critical visibility function is more of an issue. There is no guarantee we have reached the global minimum, and STEAM-ROLLER did fall into a local minimum from time to time. One should, therefore, treat all the results in this paper in the following way; it is guaranteed that a given state has a minimal critical visibility not greater than the one presented. As for the likelihood that it is also not smaller, we can only state that there's a good chance it is because STEAM-ROLLER provided us with a correct result in 99 cases out of 100.

III. BOUNDS ON LOCAL REALISM

We applied the numerical method to different types of quantum states, which are often discussed in the context of quantum information studies, namely,

• the generalized GHZ state [17, 18]: $|\mathrm{GHZ}(\alpha)\rangle_N = \cos\alpha |0\cdots 0\rangle_N + \sin\alpha |1\cdots 1\rangle_N,$

• the W state [19]:

$$|\mathbf{W}\rangle_N = \frac{1}{\sqrt{N}}(|10\cdots 0\rangle_N + |010\cdots 0\rangle_N + \cdots + |0\cdots 01\rangle_N),$$

• the four-qubit singlet state [7, 20]:

$$\begin{split} |\Psi_4\rangle &= \frac{1}{\sqrt{3}}(|0011\rangle + |1100\rangle) \\ &- \frac{1}{\sqrt{12}}(|0101\rangle + |0110\rangle + |1001\rangle + |1010\rangle), \end{split}$$

• the six-qubit singlet state [20, 21]:

$$|\Psi_6\rangle = \frac{1}{\sqrt{2}}|GHZ^-\rangle_6 + \frac{1}{2}(|\overline{W}\rangle_3|W\rangle_3 - |W\rangle_3|\overline{W}\rangle_3),$$

where $|GHZ^{-}\rangle_{6} = \frac{1}{\sqrt{2}}(|000111\rangle - |111000\rangle)$, and $|\overline{W}\rangle_{3}$ is the spin-flipped $|W\rangle_{3}$,

• the symmetric Dicke state [22]:

$$|D_N^{(N/2)}\rangle = \binom{N}{N/2}^{-1/2} \sum_{\text{permutations}} |0 \cdots 0 \underbrace{1 \cdots 1}_{N/2} 0 \cdots 0\rangle_N,$$

• the four-qubit cluster state [23]:

$$|\mathrm{Cluster}\rangle = \frac{1}{2}(|0000\rangle + |0011\rangle + |1100\rangle - |1111\rangle).$$

We calculated the critical visibility for an increasing number of different settings per side. All results are presented in Tab. I. They lead to the following observations.

Observation 1. An explicit form of tight Bell inequalities for probabilities is known only for the following experimental situations: 2x2 [24], 3x3 [25, 26], 2x2x2 [25, 26], whereby ixj means i(j) alternative measurements on Alice's (Bob's) side. In these cases the numerical method gives the same critical visibility as the analytical expressions. For states (#1 - #5) (see Tab. I) we observe such a correspondence.

Observation 2. Local realistic correlations in the N-qubit experiments with two alternative measurement settings per side are bounded by WWWZB inequalities [6, 7, 10]. In this case, the numerical method should give better or at least the same results. We obtain the same results for the following states: $GHZ(\pi/4)_N$ (#1, #2, #13, #31, #35, #39), Ψ_4 (#21), $D_4^{(2)}$ (#25), Cluster₄ (#29), Ψ_6 (#37), $D_6^{(3)}$ (#38). Stronger constraints on local realism than predicted by the WWWZB inequalities are observed for the following states:

- $|W\rangle_N$ (#17, #33, #36, #40). The corresponding critical visibilities obtained by means of WWWZB inequalities are equal to: $v_{W_3}^{crit} = 0.6565$, $v_{W_4}^{crit} = 0.6325$, $v_{W_5}^{crit} = 0.6202$, $v_{W_6}^{crit} = 0.6141$, and $v_{W_7}^{crit} = 0.6089$, and are higher than obtained by the numerical method by about 2% (for N=3) to 208% (for N=7). The values (#5, #17, #33) were previously published in [27].
- GHZ($\pi/12$)_N (#3), GHZ($\pi/180$)_N (#4). These states do not violate WWWZB inequalities at all [18, 28].

One of the simplest examples showing the advantage of Bell inequalities based on probabilities over correlation functions is a three qubit state, which is the product of the two qubit singlet state and white noise $|\psi^-\rangle_{ab}\langle\psi^-|\otimes \mathbb{1}_c$. The state does not violate the WWWZB inequalities

No.	N	State	$m_1 \times m_2 \times \cdots \times m_N$	v_{crit}
#1	2	$ \mathrm{GHZ}(\pi/4)\rangle_2$	2x2 - 10x10	0.7071
#2	3	$ \mathrm{GHZ}(\pi/4)\rangle_3$	2x2x2 - 5x5x5	0.5000
#3		$ \mathrm{GHZ}(\pi/12)\rangle_3$	2x2x2 - 4x4x4	0.8165
#4		$ \mathrm{GHZ}(\pi/180)\rangle_3$	2x2x2 - 3x3x3	0.9988
#5		$ W\rangle_3$	2x2x2	0.6442
#6			3x3x2	0.6330
#7			4x4x2	0.6240
#8			5x5x2	0.6236
#9			6x6x2	0.6236
#10			3x3x3	0.6048
#11			4x4x4	0.6013
#12			5x5x5	0.6007
#13	4	$ \mathrm{GHZ}(\pi/4)\rangle_4$	2x2x2x2	0.3536
#14			3x3x3x2	0.3536
#15			4x4x4x2	0.3536
#16			3x3x3x3	0.3408
#17		$ W\rangle_4$	2x2x2x2	0.5469
#18			3x3x3x2	0.5011
#19			4x4x4x2	0.4923
#20			3x3x3x3	0.4900
#21		$ \Psi_4 angle$	2x2x2x2	0.5303
#22			3x3x3x2	0.5012
#23			4x4x4x2	0.4948
#24			3x3x3x3	0.4823
#25		$ D_4^{(2)}\rangle$	2x2x2x2	0.4714
#26			3x3x3x2	0.4646
#27			4x4x4x2	0.4630
#28			3x3x3x3	0.4393
#29		$ \text{Cluster}\rangle_4$	2x2x2x2	0.5000
#30			3x3x3x3	0.4472
#31	5	$ \mathrm{GHZ}(\pi/4)\rangle_5$	2x2x2x2x2	0.2500
#32			3x3x3x3x3	0.2280
#33		$ W\rangle_5$	2x2x2x2x2	0.4300
#34			3x3x3x3x3	0.3462
#33		$ \text{Cluster}\rangle_5$	2x2x2x2x2	0.3333
#34			3x3x3x3x3	0.3333
#35	6	$ \mathrm{GHZ}(\pi/4)\rangle_6$	2x2x2x2x2x2	0.1768
#36		$ W\rangle_6$	2x2x2x2x2x2	0.2927
#37		$ \Psi_6 angle$	2x2x2x2x2x2	0.3536
#38		$ D_6^{(3)}\rangle$	2x2x2x2x2x2	0.2827
#39	7	$ \mathrm{GHZ}(\pi/4)\rangle_7$	2x2x2x2x2x2x2	0.1250
#40		$ W\rangle_7$	2x2x2x2x2x2x2	0.1975

TABLE I. The critical visibilities for various types of quantum states and experimental situations (number of settings). If $v > v_{crit}$, there does not exist any local realistic model describing quantum probabilities of experimental events.

for three qubits, whereas the numerical method detects violation of local realism and gives the critical visibility equal to 0.7071. This number is equivalent to the visibility, which is necessary to violate the Clauser-Horne inequality by the $|\psi^-\rangle_{ab}$ state alone. The advantage comes from the fact that probability methods use the whole knowledge obtained from an experiment.

Observation 3. Explicit forms of tight correlation function Bell inequalities [29] for three qubits and three settings per side were given in [30]. The numerical method gives the same result in (#2). In the case of (#3, #4), the inequalities of [30] are not violated. The critical visibility for violation of the inequalities by the W₃ state (#5) is equal to 0.6547 (about 2% above the visibility predicted by the numerical method).

Observation 4. Explicit forms of tight correlation function Bell inequalities for many qubits (N>3) and many measurement settings $(m_i>2)$ are still unknown. Tight Bell inequalities were constructed for some particular cases (e.g. $2^{N-1}x2^{N-1}x2^{N-2}x\dots x2$ [31]) only. There is also the family of the correlation Bell inequalities for many qubits and an arbitrary number of settings [32]. Unfortunately, these inequalities are not tight. In this case, the numerical method gives the strongest known constraints on a local realistic description.

- First, let us consider the 4x4x2-type inequality of [31]. It is violated by the $GHZ(\pi/4)_3$ state with a critical visibility equal to 0.3536 which agrees with (#2). However, for the W_3 state the inequality is violated if the visibility is higher than 0.6547 [31], whereas the numerical method reveals the critical visibility to be lower by about 4.9% (#7).
- One can also compare the numerical method with so called geometric inequalities [32]. For instance, the critical visibility of the four qubit GHZ state to violate the three-setting geometrical inequality $v_{geom}^{GHZ_4} = 0.3421$ is close to (but higher than) that expected by the numerical method (#16). However, for the four-qubit W state the three-setting geometrical inequalities are violated with a critical visibility $v_{geom}^{W_4} = 0.6843$, whereas the numerical method provides a drastically (about 28%) better result (#20).

Observation 5. One can conjecture that the critical visibility for the three-qubit W state for an arbitrary large number of settings is equal to 6/10~(#12).

Observation 6. In many cases, the critical visibility for impossibility of a local realistic description decreases with the number of settings. The highest visibility drop (19%) is observed for the five-qubit W state (#33, #34), 10% for the four-qubit W state (#17, #20), and less for W₃ (#5, #10 - #12), $GHZ(\pi/4)_4$ (#13, #16), $GHZ(\pi/4)_5$ (#31, #32), $Cluster_4$ (#29, #30), Ψ_4 (#21, #24), and $D_4^{(2)}$ (#25, #28). Interestingly, for two- and three-qubit GHZ states we do not observe this effect. Acording to [33] it could be that the effect appears with higher numbers of measuremaent settings.

Observation 7. The minimal number of measurement settings determines a lower bound on the critical visibility. In (#5 - #10, #13 - #16, #17 - #20, #21 - #24, #25 - #28) the last observer has only two alternative measurement settings. Increasing the number of measurement settings at the other sides does not result in the decrease of the critical visibility below the value for three settings per each observer.

Observation 8. The N-qubit $\mathrm{GHZ}(\pi/4)$ state reveals the strongest non-classical properties (the lowest critical visibility for an arbitrary number of $N \leq 8$). However, one can observe that the difference between the critical visibility for the GHZ state and the W state (or the cluster state) decreases with the number of qubits. According to [27], we know that the W state leads to stronger nonclassicality than GHZ states for N > 10. Finding an example for $N \leq 10$ is still an open problem. Due to computer power limitations, we were not able to recover the result of Sen et. al or find another one for $N \sim 10$.

A. Bound entanglement

We also analyze some classes of bound entangled states, namely,

• the three qubit Bennett state [34]:

$$\rho_{\text{Bennett}} = \frac{1}{4} (\mathbb{1} - \sum_{i=1}^{4} |\phi_i\rangle\langle\phi_i|),$$

where
$$|\phi_1\rangle = |01+\rangle, |\phi_2\rangle = |1+0\rangle, |\phi_3\rangle = |+01\rangle, |\phi_4\rangle = |---\rangle, |\pm\rangle = (|0\rangle \pm |1\rangle)/\sqrt{2},$$

• the N-qubit Dür state [35]:

$$\rho_N^{\text{Dür}} = \frac{1}{N+1} \left(|\phi\rangle\langle\phi| + \frac{1}{2} \sum_{k=1}^N (P_k + \tilde{P}_k) \right)$$

with $|\phi\rangle = \frac{1}{\sqrt{2}} [|0\rangle_1...|0\rangle_N + e^{i\alpha_N}|1\rangle_1...|1\rangle_N]$, and P_k being a projector on the state $|0\rangle_1...|1\rangle_k...|0\rangle_N$ with "1" on the kth position $(\tilde{P}_k$ is obtained from P_k after replacing "0"s by "1"s and vice versa),

• the generalized N-qubit Smolin state [36]:

$$\rho_N^{\text{Smolin}} = \frac{1}{2^N} \left[\mathbb{1}^{\otimes N} + (-1)^{N/2} \sum_{i=1}^3 \sigma_i^{\otimes N} \right],$$

where σ_i are the Pauli matrices.

The results are presented in Tab. II and lead to the following observations.

Observation 9. Violation of local realism by the bound entangled Smolin state (for four and six qubits). The critical visibilities obtained by the numerical method (#43, #47) recover the results of [36]. If we go to three alternative settings per side, the critical visibility for the four qubit Smolin state decreases (#44).

No. N	state	$m_1 \times m_2 \times \cdots \times m_N$	v_{crit}
#41 3	$ Bennett\rangle_3$	2x2x2 - 5x5x5	1.0000
#42 4	$ \mathrm{D\ddot{u}r}\rangle_4$	2x2x2x2 - 3x3x3x3	1.0000
#43	$ \mathrm{Smolin}\rangle_4$	2x2x2x2	0.7071
#44		3x3x3x3	0.6986
#45 5	$ \mathrm{D\ddot{u}r}\rangle_{5}$	2x2x2x2x2 - 3x3x3x3x3	1.0000
#46 6	$ \mathrm{D\ddot{u}r}\rangle_{6}$	2x2x2x2x2x2	1.0000
#47	$ \mathrm{Smolin}\rangle_6$	2x2x2x2x2x2	0.7071
#48 7	$ \mathrm{D\ddot{u}r}\rangle_7$	2x2x2x2x2x2x2	1.0000

TABLE II. The critical visibilities for some bound entangled states and experimental situations (number of settings). If $v > v_{crit}$, there does not exist any local realistic model describing quantum probabilities of experimental events.

Observation 10. In [32, 35, 37] the problem of the violation of Bell-type inequalities by the Dür state is considered. A simple experimental situation involves 7 qubits and 3 settings [37], 6 qubits and 5 settings [32], or 8 qubits and 2 settings per side [35]. We only verified the case of 7 qubits (#48). Using the numerical method we can not find a violation of a local realistic model for two settings per side. It suggests that the requirement of three settings is reasonable. We also partially verified the cases of 4 (#42), 5 (#45) and 6 (#46) qubits. We can not find a local realistic model for two measurement settings per side (and three setting in the case of 4 and 5 qubits). The problem of a violation of local realism by predictions of the four and five qubit Dür state, and the six qubit Dür state with the number of measurement settings less than 5 is still an open question.

Exemplarily, in App. B we give a local realistic model for quantum probabilities in a Bell experiment for the four qubit Dür state. The observers choose between two measurement settings which are optimal for the case of the GHZ state.

IV. FROM DETECTOR CLICKS TO DENSITY MATRIX

In this section we use the numerical method for experimentally observed states. To this end, we need their density matrices. Methods that are used to obtain the density matrix from the measured data are called quantum state tomography. Different ways for quantum state tomography have been developed (one of the first works was [38]; a variety of methods is summarized in [39]). From a decomposition of the density matrix into projectors, one can easily express the density matrix in terms of probabilities for detecting a certain coincidence. Relative frequencies obtained in a measurement are, however, subject to Poissonian counting statistics. Because of these uncertainties, the deduced density matrices might be unphysical, e.g. one might find negative eigenvalues. Such raw data are not useful for the numerical method and

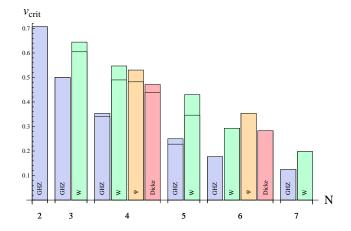


FIG. 1. (Color online) The bars represent for several families of quantum states the critical visibilities, which are necessary to falsify a local realistic description in two setting experiments. The additional line in some cases corresponds to the value of the critical visibility in a three setting experiment.

lead to the violation of local realism with visibility equal to 0, as spurious signaling-like effects may lurk in the raw data (due to experimental drifts). Fortunately, several different approaches for fitting a general physical density matrix to the measured data have been developed. There are, however, still discussions about the best method.

We apply the numerical method to the data obtained in the four-photon experiment reported in Refs. [40–42]. Spontaneous parametric down conversion in combination with linear optics was used to observe a variety of four-photon entangled states:

$$|\psi(\gamma)\rangle = \frac{1}{2}\gamma(|01\rangle + |10\rangle)^{\otimes 2} + \sqrt{\frac{1-\gamma^2}{2}}(|0011\rangle + |1100\rangle). \tag{9}$$

We select three of these states, namely, $|\psi(0)\rangle \equiv |GHZ(\pi/4)\rangle_4$, $|\psi(1/3)\rangle \equiv |\Psi_4\rangle$, $|\psi(2/3)\rangle \equiv |D_4^{(2)}\rangle$. Moreover, two further states, namely: $|GHZ(\pi/4)\rangle_2$ and $|W\rangle_3$ are obtained from the state $|\psi(2/3)\rangle$ after projective measurements. The experimental states were deduced from a full quantum state tomography with a maximum-likelihood estimation [43] of the most likely density matrix to have led to the observed data.

The STEAM-ROLLER was used to determine the critical parameter v_{crit}^{exp} for the tomographically reconstructed states (see Tab. III). If $v_{crit}^{exp} < 1$, the experiment cannot be described by any local realistic model. The critical parameters v_{crit}^{exp} can be compared with theoretical ones v_{crit}^{theor} obtained for ideal states. The critical visibility in the experiment is always larger than the theoretical one. This is due to the non-ideal preparation of the states in the experiment, which essentially reduces the non-classical correlations. Further, the ratios $v_{crit}^{theor}/v_{crit}^{exp}$ are slightly greater than the experimental fidelity of a given state, e.g. for the Dicke state (#57) $v_{crit}^{theor}/v_{crit}^{exp}=0.86$,

No. N	State	$m_1 \ge m_2 \ge \cdots \ge m_N$	v_{crit}^{theor}	v_{crit}^{exp}
#49 2	$ \mathrm{GHZ}(\pi/4)\rangle_2$	2x2	0.7071	0.7751
#50		3x3	0.7071	0.7737
#51 3	$ W\rangle_3$	2x2x2	0.6442	0.7534
#52		3x3x3	0.6048	0.7073
#53 4	$ \mathrm{GHZ}(\pi/4)\rangle_4$	2x2x2x2	0.3536	0.4365
#54		3x3x3x3	0.3408	0.4284
#55	$ \Psi_4 angle$	2x2x2x2	0.5303	0.5748
#56		3x3x3x3	0.4823	0.5410
#57	$ D\rangle_4^{(2)}$	2x2x2x2	0.4714	0.5501

TABLE III. The critical visibilities for some states (theor -theoretical and exp - experimental) and number of measurement settings.

whereas $F_{Dicke}^{exp} = 0.83$. This can be explained by the fact, that the noise observed in the experiment contains nonclassical correlations [44, 45].

V. CLOSING REMARKS

In this paper we used linear programming as a tool to study the non-classicality of quantum states. The detailed comparison of a number of multipartite entangled states demonstrates the power of this method even for modest computer equipment. Most of the conclusions were spelled out in the earlier sections. Here we want to stress that the overall message of the obtained data is that with more settings per observer one gets stronger violations of local realism. The strength of violation also increases with the number of qubits (see Fig. 1).

We would like to draw the attention of the reader to the peculiarity of three-qubit GHZ states. It is well known that the threshold visibility for the GHZ correlations to violate the Mermin three qubit inequality is 0.5. This inequality only considers highest order correlation functions. This threshold is very stubborn. As outlined previously, in our numerical approach we used not the correlation functions, but the full set of probabilities, for events of all orders. Still, even if one increases the number of settings from two per observer to five the stubborn threshold stays put at 0.5, see also [46]. An interesting extension of the phenomenon are four-qubit GHZ states: if one increases the number of settings from two to four for three observers only, with the last one always using two settings, the threshold visibility is 0.3536 for all such cases. The exact value seems to be $\frac{1}{2\sqrt{2}}$, as such is the analytic value for standard Bell inequalities (in the two settings per observer scenario). However in the 3x3x3x3 case, suddenly the critical visibility drops to 0.3408. All this points to some so far unexplained resistance of three-particle correlations, even within a fourparticle GHZ state, to reveal more non-classicality with an increasing number of settings. It should be an exciting task to find a reason for that behavior.

VI. ACKNOWLEDGMENTS

We acknowledge support from the EU program QAP (Contract No. 015848) and Q-ESSENCE (Contract No. 248095). J.G., W.L., and M.Ż. are supported by the MNiSW Grant no. N202 208538. W.L. is supported by the Foundation for Polish Science (KOLUMB program). W.W. acknowledges support by QCCC of the ENB. N.K. acknowledges support from the Alexander von Humboldt Foundation. The collaboration is a part of a DAAD/MNiSW program. M.Ż. thanks Nicolas Gisin for discussions on the problem studied in section IV.

Appendix A: Local realistic model for the noisy $|GHZ(\pi/4)\rangle_2$ state

The quantum probability function for the $GHZ(\pi/4)_2$ state has the following form:

$$P_{QM}(r_a, r_b | \theta_a, \phi_a; \theta_b, \phi_b)$$

$$= \cos(r_a \pi/4 + \theta_a) \cos(r_b \pi/4 + \theta_b)$$

$$+ \sin(r_a \pi/4 + \theta_a) \sin(r_b \pi/4 + \theta_b) \cos(\phi_a + \phi_b).$$
(A1)

Let us choose some arbitrary set of measurement angles: $\theta_i^j = 0, \phi_1^1 = 0; \phi_1^2 = \pi/2; \phi_2^1 = \pi/4; \phi_2^2 = 3\pi/4$ and put (A1) to (1). Then we get the set of constraints, under which the visibility function v should be maximized:

$$p_{0} + p_{1} + p_{5} + p_{4} = q_{-}$$

$$p_{2} + p_{3} + p_{7} + p_{6} = q_{+}$$

$$p_{4} + p_{5} + p_{13} + p_{12} = q_{-}$$

$$p_{6} + p_{7} + p_{14} + p_{15} = q_{+}$$

$$p_{0} + p_{2} + p_{8} + p_{10} = q_{+}$$

$$p_{1} + p_{3} + p_{9} + p_{11} = q_{-}$$

$$p_{4} + p_{6} + p_{12} + p_{14} = q_{-}$$

$$p_{5} + p_{7} + p_{13} + p_{15} = q_{+}$$

$$p_{8} + p_{9} + p_{13} + p_{12} = q_{+}$$

$$p_{10} + p_{11} + p_{14} + p_{15} = q_{-}$$

$$p_{0} + p_{2} + p_{6} + p_{4} = q_{+}$$

$$p_{1} + p_{3} + p_{7} + p_{5} = q_{-}$$

$$p_{8} + p_{10} + p_{12} + p_{14} = q_{-}$$

$$p_{9} + p_{11} + p_{13} + p_{15} = q_{+}$$

$$p_{0} + p_{1} + p_{9} + p_{8} = q_{+}$$

$$p_{2} + p_{3} + p_{11} + p_{10} = q_{-}$$
(A2)

with $q_{\pm} = (1 \pm v/\sqrt{2})/4$, $p_i \leq 1$ and $\sum_i p_i = 1$. For such a problem the numerical procedure gives the highest possible visibility $v_{crit} = 0.707107$, for which a local realistic model of (A1) exists. For such a value of $v = v_{crit}$, the local realistic model has the following form:

Note that in this example, the measurement was chosen arbitrarily (but in an optimal way). In a standard procedure, there is an additional optimization over measurement angles.

Appendix B: Local realistic model for a bound entangled state

The local realistic model for the quantum probabilities for the four-qubit Dür state is presented. The measurement angles are chosen in the optimal way for the $\mathrm{GHZ}(\pi/4)_4$ state, namely, $\theta_i^j=0 (i=1,2,3,4;j=1,2), \phi_1^1=0, \phi_1^2=\pi/2, \phi_2^1=\pi/4, \phi_2^2=3\pi/4, \phi_3^1=\pi/4, \phi_3^2=3\pi/4, \phi_4^1=\pi/4, \phi_4^2=3\pi/4$. Any other choice

of measurements does not have an impact for violation of local realism. The model has the following form:

- $p_0 = p_{15} = p_{21} = p_{26} = p_{38} = p_{41} = p_{51} = p_{60} = p_{67} = p_{76} = p_{112} = p_{127} = p_{150} = p_{153} = p_{165} = p_{170} = p_{214} = 0.0404029,$
- $p_{85} = p_{90} = p_{102} = p_{105} = p_{128} = p_{143} = p_{179} = p_{188} = p_{195} = p_{200} = p_{204} = p_{217} = p_{229} = p_{235} = p_{240} = p_{248} = p_{255} = 0.00379126,$
- $p_{197} = p_{219} = p_{226} = p_{238} = p_{245} = 0.0366117$,
- $p_{216} = p_{233} = 0.0328204$.

All other probabilities vanish.

- [1] A. K. Ekert, Phys. Rev. Lett. 67, 661 (1991).
- [2] M.Żukowski, A. Zeilinger, M.A. Horne and H. Weinfurter, Acta Phys. Pol. 93, 187 (1998).
- [3] H. Buhrman, W. van Dam, P. Hoyer, A. Tapp, Phys. Rev. A, 60, 2737 (1999).
- [4] Ernesto F. Galvao, Phys. Rev. A 65, 012318 (2001).
- [5] C. Brukner, M. Zukowski, J.-W. Pan, A. Zeilinger, Phys. Rev. Lett. 92, 127901 (2004).
- [6] R. F. Werner and M. W. Wolf, Phys. Rev. A 64, 32112 (2001).
- [7] H. Weinfurter and M. Żukowski, Phys. Rev. A 64, 010102(R) (2001).
- [8] M. Żukowski, D. Kaszlikowski, A. Baturo, J.-A. Larsson, arXiv:quant-ph/9910058.
- [9] D. Kaszlikowski, P. Gnaciński, M. Żukowski, W. Miklaszewski and A. Zeilinger, Phys. Rev. Lett. 85, 4418 (2000).
- [10] M. Żukowski, Č. Brukner, Phys. Rev. Lett. 88, 210401 (2002).
- [11] The highest order correlation function describes correlations only between all subsystems.
- [12] J. S. Bell, Pysics 1, 195 (1964).
- [13] G. B. Dantzig, Linear Programming and Extensions, Princeton University Press, Princeton, NJ (1963).
- [14] GNU Linear Programming Kit, Version 4.31. http://www.gnu.org/software/glpk/
- [15] J. A. Nelder, R. Mead, Computer Journal 7, 308 (1965).
- [16] SciPy Python scientific computing package, Version 0.7.0, http://www.scipy.org/
- [17] D. M. Greenberger, M. A. Horne, and A. Zeilinger, in Bell's Theorem, Quantum Theory, and Conceptions of the Universe, edited by M. Kafatos, Kluwer Academic, Dordrecht, 69 (1989).
- [18] V. Scarani, N. Gisin, J. Phys. A: Math. Gen. 34, 6043 (2001).
- [19] W. Dür, G. Vidal, J. I. Cirac, Phys. Rev. A 62, 062314 (2000).
- [20] A. Cabello, Phys. Rev. A 68, 012304 (2003).
- [21] M. Radmark, M. Żukowski, M. Bourennane, Phys. Rev. Lett. 103, 150501 (2009).
- [22] R. H. Dicke, Phys. Rev. 93, 99 (1954).

- [23] H. J. Briegel and R. Raussendorf, Phys. Rev. Lett. 86, 910 (2001).
- [24] J. F. Clauser and M. A. Horne, Phys. Rev. D 10, 526 (1974).
- [25] I. Pitowsky and K. Svozil, Phys. Rev. A 64, 014102 (2001).
- [26] C. Śliwa, Phys. Lett. A 165, 3 (2003).
- [27] A. Sen(De), U. Sen, M. Wieśniak, D. Kaszlikowski, and M. Żukowski, Phys. Rev. A 68, 062306 (2003).
- [28] M. Żukowski, Č. Brukner, W. Laskowski, M. Wieśniak, Phys. Rev. Lett. 88, 210402 (2002).
- [29] Tight Bell inequalities define the half-spaces in which is the correlation (local realistic) polytope, which contain a face of it in their border hyperplane.
- [30] M. Wieśniak, Marek Zukowski, Phys. Rev. A 76 012110 (2007).
- [31] W. Laskowski, T. Paterek, M. Žukowski, Č. Brukner, Phys. Rev. Lett. 93, 200401 (2004).
- [32] K. Nagata, W. Laskowski, T. Paterek, Phys. Rev. A 74, 062109 (2006).
- [33] T. Vértesi, Phys. Rev. A 78, 032112 (2008).
- [34] C.H. Bennett, D.P. DiVincenzo, T. Mor, P.W. Shor, J.A. Smolin, B.M. Terhal, Phys.Rev.Lett. 82 5385 (1999).
- [35] W. Dür, Phys. Rev. Lett. 87, 230402 (2001).
- [36] R. Augusiak, P. Horodecki, Phys. Rev. A 73, 012318 (2006).
- [37] D. Kaszlikowski, L. C. Kwek, J. Chen, and C. H. Oh, Phys. Rev. A 66, 52309 (2002).
- [38] D.F.V. James, P.G. Kwiat, W.J. Munro and A.G. White, Phys. Rev. A 64, 052312 (2001).
- [39] J. Rehacek and M.G.A. Paris: Lecture Notes in Physics: Quantum State Estimation, Springer, 2004.
- [40] W. Wieczorek, Ch. Schmid, N. Kiesel, R. Pohlner, O. Gühne, and H. Weinfurter, Phys. Rev. Lett. 101, 010503 (2008).
- [41] W. Wieczorek, N. Kiesel, C. Schmid, W. Laskowski, M. Zukowski and H. Weinfurter, IEEE J. Sel. Top. Quant. Electron. 15, 1704 (2009).
- [42] M. Aspelmeyer and J. Eisert, Nature 455 180 (2008).
- [43] Z. Hradil, Phys. Rev. A 55, R1561 (1997).
- [44] W. Laskowski, M. Wieśniak, M. Żukowski, M. Bourennane, H. Weinfurter, J. Phys. B 42, 114004 (2009).

- [45] W. Wieczorek, N. Kiesel, C. Schmid, and H. Weinfurter, Phys. Rev. A 79, 022311 (2009).
- [46] Unfortunately, at the moment we cannot extend our investigations to more settings than 5. This is because of the memory requirements of the program and speed of

the machine. Further, we cannot be 100% certain that the algorithm reaches the global minimum. Still, the program is constructed in such a way that it never gives too low values for v_{crit} . Thus, we are always on the safe side with our claims of non-classicality.